research articles Journal of proteome research

A Proteomics Approach to Identify Protein Expression Changes in Rat Liver Following Administration of 3,5,3′-Triiodo-L-thyronine

Elena Silvestri,[†,§] Maria Moreno,[†,§] Luigi Schiavo,[†] Pieter de Lange,[#] Assunta Lombardi,[+] Angela Chambery,[#] Augusto Parente,[#] Antonia Lanni,[#] and Fernando Goglia*[,†]

Dipartimento di Scienze Biologiche ed Ambientali, Università degli Studi del Sannio, Via Port'Arsa 11, 82100 Benevento, Italy, Dipartimento di Scienze della Vita, Seconda Università di Napoli, Via Vivaldi 43, 81100 Caserta, Italy, and Dipartimento delle Scienze Biologiche, Sezione Fisiologia, Università degli Studi di Napoli "Federico II", Via Mezzocannone 8, 80134 Napoli, Italy

Received April 4, 2006

We analyzed whole cell protein content of rat liver following T3 administration. Fourteen differentially expressed proteins were unambiguously identified and were involved in substrates and lipid metabolism, energy metabolism, detoxification of cytotoxic products, calcium homeostasis, amino acid catabolism, and the urea cycle. This study represents the first systematic identification of T3-induced changes in liver protein expression profile and provides novel information at the molecular, cellular, and tissue level of T3 action.

Keywords: triiodothyronine • liver • thyroid hormone action

Introduction

3,5,3′-Triiodo-L-thyronine (T3), through a broad range of actions, modulates development, growth, and metabolism.[1,2] Its binding to nuclear receptors is believed to be one of the main events in intracellular T3 signaling pathways, with the nuclear receptors acting as ligand-activated transcription factors regulating the expressions of target genes directly through DNA response elements.[3−5] In adult life, T3, among its other actions, exerts a profound effect on basal metabolic rate, increasing respiration rate and simultaneously lowering metabolic efficiency.[2] In this context, it is known that the actions of T3 on the transcription of nuclear genes lead to coordinated and synergistic effects on mitochondrial genome expression.[6] Indeed, the actions of T3 underlie a nucleus-mitochondrion cross-talk achieved through: (i) the induction of nuclear-encoded mitochondrial factors[6,7] and (ii) direct binding of T3 to specific ligand-dependent mitochondrial transcription factors.[8,9] The overall transcription-dependent T3 signaling can be modulated at many levels, including the TR isoforms present in the tissue, the DNA response element in the regulated gene, the availability of receptor binding partners, interactions with coactivators and corepressors, ligand availability, mRNA and protein stability, protein translocation, and metabolic interferences.[6−10] Furthermore, several T3-mediated post-transcriptional changes support T3 activity.[11] Thus, the network of factors and cellular events involved in T3 signaling is very complex. Moreover, the mechanisms underlying the tissue-specific actions of T3 appear even more complicated, and they remain incompletely understood.

The liver is one of the major targets of T3 and, thus, represents an ideal tissue for studying the actions exerted by this hormone on the modulation of expression patterns. The liver performs special tasks in intermediary metabolism,[12] and approximately 8% of hepatic genes are estimated to be regulated by T3 in vivo.[13] Consequently, in recent years, the liver has been thoroughly studied with a view to describing T3-modulated gene expression, either by studies of individual genes or by a large-scale gene-expression profile approach, such as cDNA microarray hybridization.[14,15] However, despite the studies on the thyroid hormone regulation of transcription, little information concerning the status of the corresponding encoded proteins has been achieved, and the ultimate effect of T3 on translation products remains largely unknown. The presence of a transcript does not necessarily reflect the protein level, and its detection does not elucidate critical issues regarding protein functionality, such as protein localization, occurrence of its partners and/or cofactors. Thus, for a more profound investigation of the biological events modulated by T3 in target organs including liver, a systematic analysis of the T3-induced charges in protein profile is appropriate. Two-dimensional gel electrophoresis (2D-E) and mass spectrometry (MS) represent two powerful proteomic tools for the study of hormone effects on cellular metabolism and protein expression since they allow simultaneous measurement and comparison of the expression levels of hundreds of proteins.[16,17] Moreover, they provide an important complement to genomic approaches, improving our view of the complex network of molecular pathways underlying the cellular adaptation to environmental/hormonal stimuli.

* Address correspondence to Prof. Fernando Goglia, Dip. di Scienze Biologiche ed Ambientali, Università degli Studi del Sannio, Via Port'Arsa 11, 82100 Benevento, Italy. Tel.: +39 0824 305108. Fax: +39 0824 23013. E-mail: goglia@unisannio.it.
† Università degli Studi del Sannio.
§ These authors contributed equally to the manuscript.
# Seconda Università di Napoli.
+ Università degli Studi di Napoli "Federico II".

10.1021/pr060141l CCC: $33.50

Published on Web 08/01/2006

To obtain a deeper insight into the molecular events modulated by T3 in the liver, we performed a high-resolution differential proteomic analysis combining 2D-E and subsequent matrix-assisted laser desorption/ionization-time-of-flight MS (MALDI-TOF MS) techniques. To this end, we injected T3 into hypothyroid rats and compared 2D-E maps of total liver extracts from these animals with those obtained from hypothyroid ones, and then identified the differentially expressed proteins. The present study is the first application of proteomic technology with the aim of studying the modulation that T3 exerts in vivo on liver proteins, and it provides the first systematic identification of T3-induced changes in the rat liver protein expression profile.

Experimental Section

Materials. 3,5,3′-Triiodo-L-thyronine (T3), propylthiouracil (PTU), and iopanoic acid (IOP) were purchased from Sigma-Aldrich Corp. (St. Louis, MO). All solvents used were of high-performance liquid chromatography (HPLC) grade (Sigma-Aldrich Corp. and Carlo Erba, Italy). Immobilized pH-gradient (IPG) and ampholites were purchased from Bio-Rad. Acrylamide, other reagents for the polyacrylamide gel preparation, CHAPS, urea, thiourea, dithioerythriol, EDTA, iodoacetamide, colloidal Coomassie blue, and trypsin were from Sigma-Aldrich. ZipTip C18 microcolumns were from Millipore (Milan, Italy).

Animals. Male Wistar rats (250−300 g) (Charles River, Lecco, Italy) were kept one per cage in a temperature-controlled room at 28 °C under a 12-h light, 12-h dark cycle. A commercial mash and water were available ad libitum. Two groups of rats (each consisting of 4 animals) were used throughout: namely, hypothyroid rats (referred to as Hypo) and T3-treated hypothyroid rats (referred to as Hypo+T3). To study the effect of T3 on the hepatic protein expression profile, we injected T3 into hypothyroid rats [in which hypothyroidism had been induced by the ip administration of PTU (1 mg/100 g BW) for 4 weeks together with a weekly ip injection of IOP (6 mg/100 g BW)[18,19]]. This treatment provided us with hypothyroid rats with low thyroid-hormone levels and an inhibition of all three of the deiodinase enzymes.[18,19] T3 was chronically administered by giving seven daily ip injections of 15 μg T3/100 g BW to hypothyroid rats, while the control hypothyroid rats received saline injections [dose and duration of T3 treatment were chosen to obtain a change in the levels of T3 without inducing a syndrome of hypermetabolism[8−20]]. This animal model allows us to exclude the effects of other active iodothyronines putatively derived from the peripheral metabolism of thyroid hormone after T3 injection. At the end of the treatment, rats were anesthetized and then killed by decapitation. Livers were excised, weighed, and immediately frozen in liquid nitrogen, then stored at −80 °C for later processing. All experiments were performed in accordance with general guidelines regarding animal experiments and were approved by our institutional committee for animal care.

Protein Extraction and Sample Preparation. For preparation of the total protein extract, liver tissue (1.0 g) was suspended in 10 mL of sample buffer consisting of 20 mM Tris, 7 M urea, 2 M thiourea, 4% CHAPS, 10 mM 1,4-dithioerythritol (DTE), 1 mM EDTA, and a mixture of protease and phosphatase inhibitors [1 mM PMSF, one tablet completeTM (Boehringer Mannheim) per 50 mL of suspension buffer, 0.2 mM Na_2VO_3, and 1 mM NaF], as previously described.[21] The suspensions were homogenized using a Polytron homogenizer, sonicated for 30 s, and centrifuged at 150 000*g* for 45 min. The obtained supernatants contained the total liver proteins solubilized in the isoelectrofocusing (IEF)-compatible agents. The protein content of each protein sample was determined by the Coomassie blue method.[22] Total protein extracts were prepared for each animal, and each individual was assessed separately.

Two-Dimensional Gel Electrophoresis (2D-E). Samples of 250 μg of protein were applied to immobilized pH 3−10 nonlinear gradient strips (11 cm). For each sample, triplicate runs were performed as independent experiments. Samples of 1 mg of protein were utilized for preparative gels (pH 3−10 nonlinear gradient strips 17 cm). Focusing started at 250 V, with the voltage being gradually increased to 8000 V and kept constant for a further 35 000 V/h (PROTEAN IEF System, Bio-Rad). Prior to SDS-PAGE, the IPG strips were incubated for 15 min with a solution of Tris-HCl buffer (pH 8.8), urea (6 M), glycerol (30%, v/v), SDS (2%, w/v), and DTT (2%, w/v). Strips were then equilibrated for another 15 min in the same buffer containing iodoacetamide (2.5%, w/v) instead of DTT. The second-dimensional separation was performed in 10% SDS-polyacrylamide gels. After protein fixation, the gels were stained with colloidal Coomassie blue, according to the manufacturer's instructions. Molecular masses were determined by running standard protein markers, covering the range 10−200 kDa. The p*I* values used were those given by the supplier of the IPG strips.

Protein Visualization and Image Analysis. Electronic images of the gels were recorded as digitized images using a calibrated densitometer (GS-800, Bio-Rad). Gel image analysis was performed using PDQuest software (Bio-Rad). Scanned gel images were processed for removal of background and automatic detection of spots. For all spot-intensity calculations, normalized values were used to calculate relative intensity (RI) for each spot: $RI = v_i/v_t$, where v_i is the volume of the individual spot, and v_t is the sum of the volumes of all matched spots. For each matchset analysis, maps corresponding to protein extracts from animals of the same thyroid status were organized into two "Replicate Groups" (each containing 4 maps), named Hypothyroid (Hypo) and T3-treated Hypothyroid (Hypo + T3), respectively. This allowed us to carry out a statistical analysis of the experimental data relative to normalized spot densities.

Statistical Analysis. Statistical analysis was performed using a Student's *t*-test. Spots for which the *P* value was less than 0.05 were considered to display significant changes.

In-Gel Digestion. In-gel digestion with trypsin was performed as described by others[23] with minor modifications. In brief, spots showing significant changes in expression level were manually excised from the 2D-E gels, and destained by washing twice with 100 μL aliquots of water and performing a further washing step with 50% acetonitrile. The gel pieces were then dried in a SpeedVac Vacuum (Savant Instruments, Holbrook, NY) and rehydrated with 10 μL of 50 mM ammonium bicarbonate, followed by the addition of 5 μL of a 70 ng/mL TPCK porcine trypsin solution. Digestion was performed by incubation at 37 °C for 3 h. Further amounts of buffer solution without trypsin were added when necessary to keep the gel pieces wet during the digestion. Peptides were extracted in two steps by sequential addition of 1% trifluoroacetic acid (TFA) and then of 2% TFA/50% acetonitrile for 5 min in a sonication bath. The combined supernatants were concentrated in the SpeedVac Vacuum for mass spectrometry analysis. When necessary, the tryptic peptide mixture was extracted and purified with Millipore ZIPTIP C18 columns (Milan, Italy).

MALDI-TOF MS Analysis. After in situ tryptic digestion, proteins were identified by peptide mass fingerprint (PMF) based on matrix-assisted laser desorption/ionization time-of-flight mass spectrometry (MALDI-TOF-MS), as follows. Tryptic peptides were mixed with an equal volume of saturated α-cyano-4-4-hydroxycinnamic acid matrix solution [10 mg/mL in ethanol/water (1:1; v/v), containing 0.1% TFA] and spotted onto a MALDI-TOF target plate. The droplet was dried at room temperature. Once the liquid was completely evaporated, the sample was loaded into the mass spectrometer and analyzed. Peptide spectra were collected on a MALDI LR mass spectrometer (Waters Corporation, Milford, MA) in the positive ion, reflectron mode. The instrument was externally calibrated using a tryptic alcohol dehydrogenase digest (Waters, Milford, MA) as standard. The protonated monoisotopic mass of Adreno Cortico Trophic Hormone (ACTH) peptide (m/z 2465.199) was used as internal lock mass to further improve the peptide mass accuracy to within 50 ppm. All spectra were processed and analyzed using the MassLynx 4.0 software (Waters, Milford, MA). The obtained spectra were used to identify proteins in the Swiss-Prot protein sequence database by using Protein Lynx Global Server 2.0 software. The following searching parameters were used: mass tolerance, 50 ppm; allowed number of missed cleavage sites up to 1; cysteine residue modified as carbamidomethyl-Cys; minimum number of matched peptides, 3; the isotope masses were used.

RT-PCR Analysis. Total RNA was prepared from frozen tissue samples by using TRIzol according to the manufacturer's protocol (Invitrogen). Total RNA (1 μg) was reverse-transcribed using 100 pmol random hexamers (Invitrogen), 2.0 units Superscript reverse-transcriptase, 0.5 units RNase inhibitor, and 1 mM deoxynucleotide triphosphates (dNTPs) in reverse-transcriptase buffer (all from HT Biotechnology, Cambridge, U.K.). The total volume was adjusted to 20 μL with sterile distilled water. The RT reaction was carried out for 1 h at 40 °C. One-quarter of the RT-reaction mixture was used directly for the PCR reaction in a total volume of 25 μL, containing 0.25 units of SuperTaq polymerase, 0.25 mM dNTPs, SuperTaq PCR buffer (all from HT Biotechnology), 5% (v/v) dimethyl sulfoxide (DMSO, Sigma-Aldrich Corp.), and 0.38 pmol of the relevant oligonucleotide primers (Primm, Italy). As an internal control, the same cDNAs were amplified using 40S ribosomal protein S12 (RPS12) oligonucleotide primers. The primers used had the following sequences: malic enzyme sense, 5′-GCCCTGAATATGATGCGTTT-3′; malic enzyme antisense, 5′-CCTGGAACAGCACTGTCTGA-3′; deiodinase type I sense, 5′-CCTCCACAGCTGACTTCCTC-3′; deiodinase type I antisense, 5′-TAGAGCCTCTCAGGCAGAGC-3′; Acyl-CoA dehydrogenase sense, 5′-ATGTGCCAGAGGAGCTGAGT-3′; Acyl-CoA dehydrogenase antisense, 5′-AAACAGCCGATTTTTGTCACC-3′; ATP Synthase α chain sense, 5′-AGGAACGTTCAAGCTGAGGA-3′; ATP Synthase α chain antisense, 5′-ACTACACGGCCCAACAGTTC-3′; Electron-transfer flavoprotein α-subunit sense, 5′-ACCTTCTGCCCAGAGTAGCA-3′; Electron-transfer flavoprotein α-subunit antisense, 5′-GCAGCCTCAAAAGATGTTCC-3′; Arginase-1 sense, 5′-TATCGGAGCGCCTTTCTCTA-3′; Arginase-1 antisense, 5′-ACAGACCGTGGGTTCTTCAC-3′. Parallel amplifications (20, 25, and 30 cycles) of a given cDNA were used to determine the optimum number of cycles. For each gene under study, a readily detectable signal within the linear range was observed after 30 cycles. For the actual analysis, samples were heated for 5 min at 95 °C, then 30 cycles were carried out, each consisting of 1 min at 95 °C, 1 min at 60 °C, and 1.0 min at 72 °C. This was followed by a final 10-min extension at 72 °C. Separation of the PCR-products was performed on a 2% agarose gel containing ethidium bromide. The products were readily visualized, and they were quantified by means of a Bio-Rad Molecular Imager FX using the supplied software (QuantityOne, Bio-Rad). Expression signals were normalized with respect to the RPS12 signal.

Results

Protein Expression Profiling by 2D-E Analysis in Rat Liver of Hypo and Hypo+T3 Rats. For each rat ($n = 4$ Hypo, $n = 4$ Hypo+T3) the liver was dissected, and proteins were extracted and separated on a 2D-E gel. Overall, the 2D-E gel protein spot patterns across all the gels were qualitatively and quantitatively similar (Figure 1A). With the detection limits set, the software counted, on average, 600 spots per gel, of which 85−95% was matched between gels in each set and subsequent analysis was conducted considering only spots present under both experimental conditions. Statistical analysis of the densitometric data allowed the identification of differentially expressed protein spots between Hypo and Hypo+T3 maps organized in replicate groups. As shown in Figure 1B, statistical analysis applied to Hypo+T3 versus Hypo maps found 53 differentially expressed spots ($P < 0.05$).

Identification of Differentially Expressed Proteins. Next, the spots differentially expressed were manually excised from relative Coomassie blue-stained preparative gels and submitted to digestion, with subsequent protein identification being performed using MALDI-TOF MS. This led to the identification of 23 differentially expressed proteins corresponding to 14 different gene products (Table 1) in accordance with the protein identification of Fountoulakis et al.[21] The molecular weight (M_r) and isoelectric point (pI) of all of these proteins correspond roughly to their position on the 2D-E gel. Furthermore, several proteins were identified at multiple spot positions (e.g., glutathione-S-transferase), putatively reflecting the occurrence of post-translational modifications. In these cases, however, on average, the variation of the spots was similar (Table 1).

Functional Grouping of Proteins Differentially Expressed Following T3 Administration. T3 administration led to the identification of 14 proteins (4 up-regulated and 10 down-regulated) that were differentially expressed in liver ($P < 0.05$) (see Table 1).

On the basis of the identities of these proteins, we grouped them into five functional categories: (i) substrates and lipid metabolism, (ii) energy metabolism, (iii) detoxification of cytotoxic products, (iv) calcium homeostasis, and (v) amino acids catabolism and the urea cycle.

(i) Substrates and Lipid Metabolism. Consistent with some of the established metabolic effects of thyroid hormone, T3 regulated several proteins known to affect many different pathways of substrate metabolism. These included enzymes involved in ethanol utilization, glucose metabolism, fatty acid oxidation, and NAD^+ biosynthesis.

In particular, spots 25 and 27 (Figure 1B), corresponding to aldehyde-dehydrogenase and α-enolase, were significantly up-regulated following T3 administration (125 and 240% increase, respectively) (Table 1, Figure 2A,B).

In contrast, negative modulations by T3 were detected for spots 32, 37, 38, and 46 (Figure 1B), corresponding to 3-keto-acyl-CoA thiolase (Figure 2C), acyl-CoA dehydrogenase, sorbitol dehydrogenase (Figure 2D), and hydroxyanthranilate 3,4-

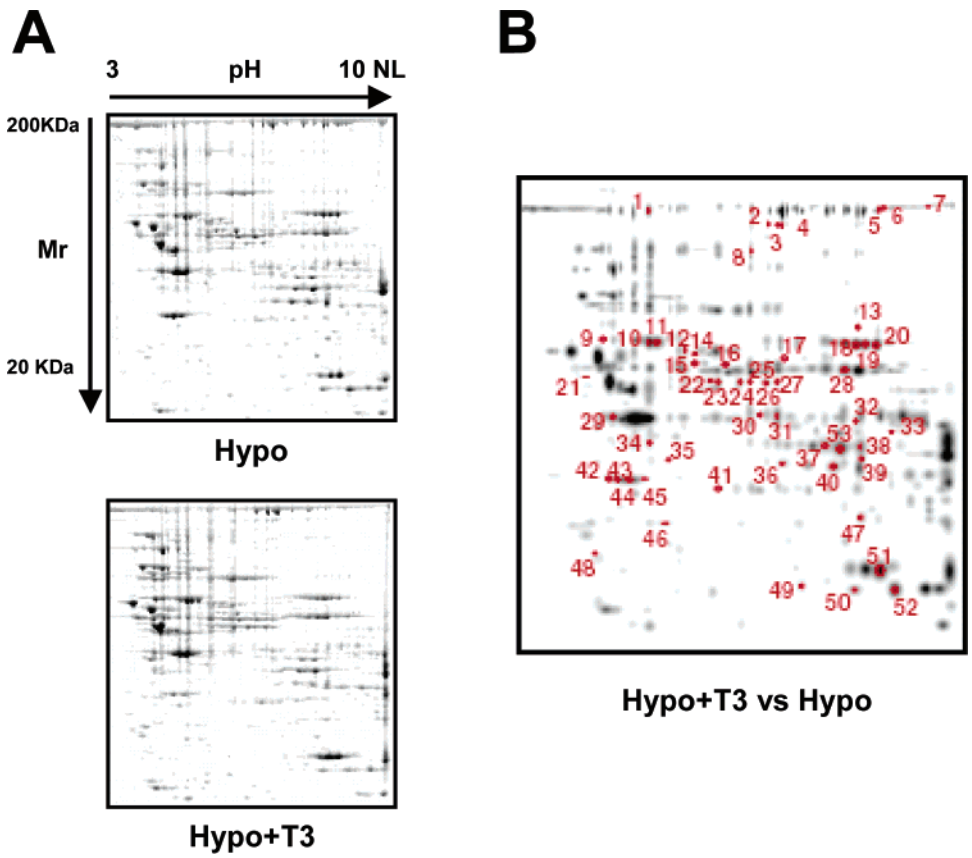

Figure 1. (A) Representative 2D-E images obtained from livers of Hypo and Hypo+T3 rats. 2D-E was performed using a nonlinear pH range of 3−10 in the first dimension (11 cm strips) and SDS-PAGE (10%) in the second. Protein loading was 250 μg, and the gels were stained using Colloidal Coomassie blue. Calibration of M_r and p*I* was performed using PDQuest software. (B) Differentially expressed proteins in livers of Hypo+T3 rats vs Hypo ones. Protein spots for which density was significantly different ($P < 0.05$) between the two thyroid states are marked in the master gel of the relative matchset. Numbers marked on the gel indicate the spots automatically counted by the PDQuest software.

dioxygenase, their protein expression levels being decreased by 50, 39, 52, and 59%, respectively (Table 1).

(ii) Energy Metabolism. It is well-established that T3 has a stimulatory effect on energy metabolism involving the mitochondrial energy transduction apparatus. Here, we report that T3 induced a significant up-regulation (50% increase) of spot 28, corresponding to ATP synthase α chain (Figure 1B; Table 1; Figure 2E), and that it significantly reduced (26% decrease) the expression level of spot 47, corresponding to electron-transfer flavoprotein α subunit (Figure 1B; Table 1; Figure 2F).

(iii) Detoxification of Cytotoxic Products. T3 accelerates hepatic respiration while concomitantly increasing ROS production and decreasing antioxidant defenses, leading to enhanced oxidative stress. Our data reveal that several enzymes involved in the detoxification of cytotoxic products were affected by T3 administration. In particular, spots 18−20 (Figure 1B), corresponding to peroxisomal catalase, were decreased by 58% (Table 1 and Figure 3A). Similarly, spots 50−52, corresponding to glutathione-S-transferase, were decreased by 58% following T3 treatment (Table 1 and Figure 3B). On the other hand, T3 administration, up-regulated spots 10 and 11 corresponding to molecular chaperone heat shock protein 60 (180 and 40% increase, respectively) (Table 1 and Figure 3C).

(iv) Calcium Homeostasis. Among the factors involved in the actions of thyroid hormone, calcium plays a major role. Calcium-binding protein regucalcin, also known as senescence marker protein 30 (SMP30), previously not known to be a T3 target, was here identified as being responsive to T3 treatment. Indeed, spots 43 and 44, identified as SMP30, were significantly down-regulated (51% decrease) in the Hypo+T3 maps (Table 1 and Figure 4A).

(v) Amino Acid Catabolism and the Urea Cycle. Several enzymes involved in amino acid metabolism are regulated by thyroid hormone. Here, we report that T3 induced significant reductions in the expression level of spots 40 and 53 (Figure 1B), corresponding to ornithine carbamoyltransferase (involved in the second step in the urea cycle) (65% decrease) and arginase-1 (involved in the first step in the arginine degradation pathway) (40% decrease), respectively (Table 1; Figure 4B,C).

To deeper investigate on the significance of the <2-fold changes that we observed for some of the identified proteins, we checked for the association of these changes with similar or dissimilar changes in the relative mRNA expression following T3 treatment. RT-PCR measurements for acyl-CoA dehydrogenase and ATP synthase α chain revealed that mRNA expression levels of both enzymes paralleled those of the corresponding proteins (Figure 5). On the other hand, mRNA expression levels of both α-ETF and arginase-1 in Hypo+T3 livers versus Hypo ones resulted to be not in accordance with protein expression levels, being significantly up-regulated following T3 treatment (Figure 5).

Table 1. Differentially Expressed Proteins in Liver of Hypo+T3 Rats versus Hypo Ones[a]

spot no.	protein name	accession no.*	theoretical M_r/pI	%Pr	sequence coverage	$P \leq 0.05$	fold change Hypo+T3 vs HYpo
	Substrate and Lipid Metabolism						
25	Aldehyde-dehydrogenase	P81178	54.30/6.0	70.5	10.8	$P < 0.05$	2.24
27	α-enolase	P04764	46.95/6.5	64.8	48.3	$P < 0.05$	3.40
32	3-ketoacyl-CoA thiolase, mitochondrial	P13437	42.24/7.92	99.8	31.2	$P < 0.05$	0.50
37	Acyl-CoA dehydrogenase, short chain-specific, mitochondrial precursor	P15651	45.02/8.34	99.8	20.5	$P < 0.05$	0.61
38	Sorbitol dehydrogenase	P46953	32.84/5.71	99.8	31.2	$P < 0.02$	0.48
46	3-hydroxyanthranilate 3,4-dioxgenase	P27867	43.37/7.22	99.8	41.1	$P < 0.05$	0.41
	Energy Metabolism						
28	ATP synthase α chain, mitochondrial precursor	P15999	58.90/10.1	99.8	41.3	$P < 0.05$	1.50
47	Electrontransfer flavoprotein α-subunit, mitochondrial precursor	P13803	35.24/8.60	99.8	31.2	$P < 0.01$	0.74
	Detoxification						
10	Heat shock protin 60	P19226	60.92/6.1	96.3	44.0	$P < 0.01$	2.80
11	Heat shock protin 60	P19226	60.92/6.1	98.6	41.0	$P < 0.05$	1.50
18	Catalase	P04762	59.58/7.5	98.6	41.1	$P < 0.01$	0.42
19	Catalase	P04762	59.58/7.5	99.8	31.2	$P < 0.01$	0.48
20	Catalase	P04762	59.58/7.5	100	20.5	$P < 0.02$	0.52
48	Catalase	P04762	59.58/7.5	99.6	41.3	$P < 0.05$	0.42
50	Glutathione-S-transferase	P04905	25.77/8.5	100	76.0	$P < 0.05$	0.35
51	Glutathione-S-transferase	P04905	25.77/8.5	96.3	70.0	$P < 0.05$	0.67
52	Glutathione-S-transferase	P04905	25.77/8.5	99.8	76.0	$P < 0.02$	0.31
	Calcium Homeostasis						
43	Senescence marker protein 30	Q03336	33.37/5.5	100	44.5	$P < 0.05$	0.34
44	Senescence marker protein 30	Q03336	33.37/5.5	99.8	41.2	$P < 0.02$	0.49
	Amino Acid Catabolism and Urea Cycle						
40	Ornithine carbamoyltransferase, mitochondrial precursor	P00481	39.92/9.91	99.8	41.1	$P < 0.05$	0.35
53	Arginase-1	P07824	34.95/7.2	80.9	64.1	$P < 0.05$	0.68

[a] Identified proteins were grouped into broad functional categories. Total liver proteins were extracted, separated by 2D-E, and identified by MALDI-TOF MS, following in-gel digestion with trypsin. The search in the Swiss-Prot protein sequence database was performed using Protein Lynx Global Server 2.0 software. At least 3 matching peptides were required for an identity assignment. "Spot no." refers to spot numbers indicated in Figure 1B. *, Swiss-Prot accession number. The theoretical M_r and pI are given. %Pr represents the identification probability, and the sequence coverage is given. Differential expression ($P < 0.05$ in Student's t-test) is given as the fold change. Values were calculated by comparing the mean relative intensity (RI) of each spot between Hypo+T3 and Hypo signals within the same experiment (representative analysis set, $n = 4$).

Discussion

By applying a proteomic approach, we have here characterized the protein expression changes that occur in the liver following administration of T3 to hypothyroid rats, in effect mapping the in vivo T3-associated modulation of proteome, likely due to T3 influence on gene transcription, mRNA and protein stability, and translation. Following T3 administration, we identified differentially expressed proteins and grouped them into the five functional categories described below. As "classical" targets of T3 were not identified in the analyzed maps, to verify liver responsiveness to T3-treatment, we measured the mRNA expression levels of malic enzyme[24] and deiodinase type 1.[25] As expected, for both enzymes, the mRNA levels were significantly up-regulated in Hypo+T3 livers (data not shown), thus, confirming the thyroid state of the examined tissues.

Substrate and Lipid Metabolism. T3 modulates several enzymes involved in substrate metabolism. Our data demonstrate that T3 treatment affects the expressions of enzymes such as mitochondrial aldehyde dehydrogenase, α-enolase, sorbitol dehydrogenase, acyl-CoA dehydrogenase, 3-ketoacyl-CoA thiolase, and 3-hydroxyanthranilate 3,4-dioxygenase. Interestingly, the first two enzymes were up-regulated, while the others were down-regulated. Mitochondrial aldehyde dehydrogenase belongs to the aldehyde dehydrogenase family,[26] and its activity produces NADH by oxidation of an aldehyde. It catalyzes the second step of ethanol utilization, and in addition, it is directly implicated in the detoxification of mitochondrial reactive aldehydes,[27] formed mainly by lipid peroxidation and deleterious for mitochondrial function. Our data are in accordance with the role played by thyroid hormone in the stimulation of the rate of ethanol elimination[28,29] and provide further insight into the mechanisms actuated by T3 in such a pathway. T3 is known to stimulate gluconeogenesis and glucose production in the liver, thereby opposing the action of insulin on hepatic glucose production.[30] Our results extend this knowledge by showing that T3 significantly enhances the level of α-enolase, which catalyses the reversible dehydration of 2-phosphoglycerate to phosphoenolpyruvate, thereby participating in glycolysis and gluconeogenesis. As previously observed in rat skeletal and cardiac muscle development[31] or in human fibroblast,[32] we report a T3-induced modulation of α-enolase protein in liver. Actually, modulation of enolase isozymes has been reported during rat skeletal and cardiac muscle development[31] and, more recently, in human fibroblasts.[32] In this context, our data on the protein level of α-enolase together with that of sorbitol dehydrogenase, the second enzyme in the polyol pathway, support the ability of T3 to inhibit glycolysis and stimulate gluconeogenesis. Moreover, it was previously reported that hyperthyroidism is associated in the liver with a reduction in sorbitol dehydrogenase activity.[33] As a whole, these data extend the previously obtained findings on the complex pattern of action of T3 in vivo on substrate metabolism and, at the same time, highlight the T3-induced down-regulation of several novel proteins in the liver.

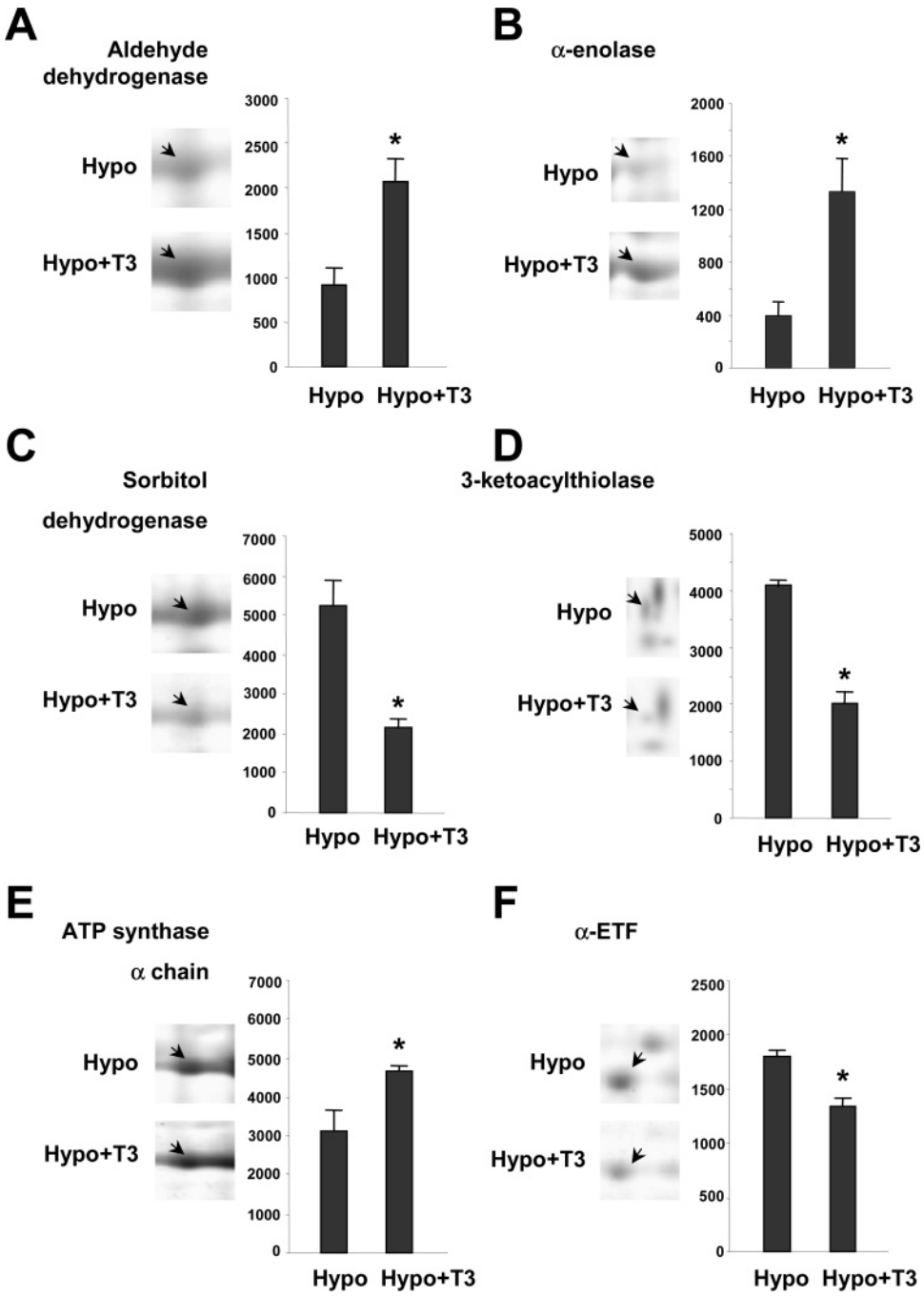

Figure 2. Example of differential expression of liver proteins involved in substrate and energy metabolism. Representative subsections of 2D-E images are shown for: (A) aldehyde dehydrogenase; (B) α-enolase; (C) sorbitol dehydrogenase; (D) 3-ketoacylthiolase; (E) ATP synthase α-chain; (F) electron-transfer flavoprotein α-subunit, mitochondrial precursor (α-ETF). In each panel, histograms show means ± SE ($n = 4$) for relative intensities (RI) of the protein spots obtained for Hypo and Hypo+T3 rats. * $P < 0.05$ vs Hypo.

T3 simultaneously stimulates mitochondrial uptake of long-chain fatty acids via the carnitine palmitoyl transferase (CPT) system, β-oxidation, and ketogenesis.[34] Here, we show that T3 induces a down-regulation of both short chain-specific acyl-CoA dehydrogenase and 3-ketoacyl-CoA thiolase, which are mitochondrial enzymes of the fatty acid β-oxidation system. Acyl-CoA dehydrogenase, in particular, catalyses the first step in the pathway and individuates a family of homologous flavoproteins [the acyl-CoA dehydrogenase (ACD) family[35]] with different specificities: short chain (SCAD), medium chain (MCAD), and long chain acyl-CoA dehydrogenases (LCAD). Each of these enzymes catalyses the formation of 2-enoyl-CoA from the saturated ester[36] and has high affinities both for its acyl-CoA substrates and for its enoyl-CoA products, resulting in product inhibition.[37−39] Low levels of SCAD and the parallel down-regulation of 3-ketoacyl-CoA thiolase following T3 administration would suggest a T3-induced modulatory effect serving to optimize the flux of fatty acids through β-oxidation.

Energy Metabolism. Thyroid hormones are regulators of cellular respiration, with mitochondria being a major target.[40−42] Here, we provide the first evidence that T3 induces a significant increase in the hepatic ATP synthase α-chain content, in accordance with the ability of T3 to stimulate ATP synthesis. On the other hand, we also show that T3 induces a reduction

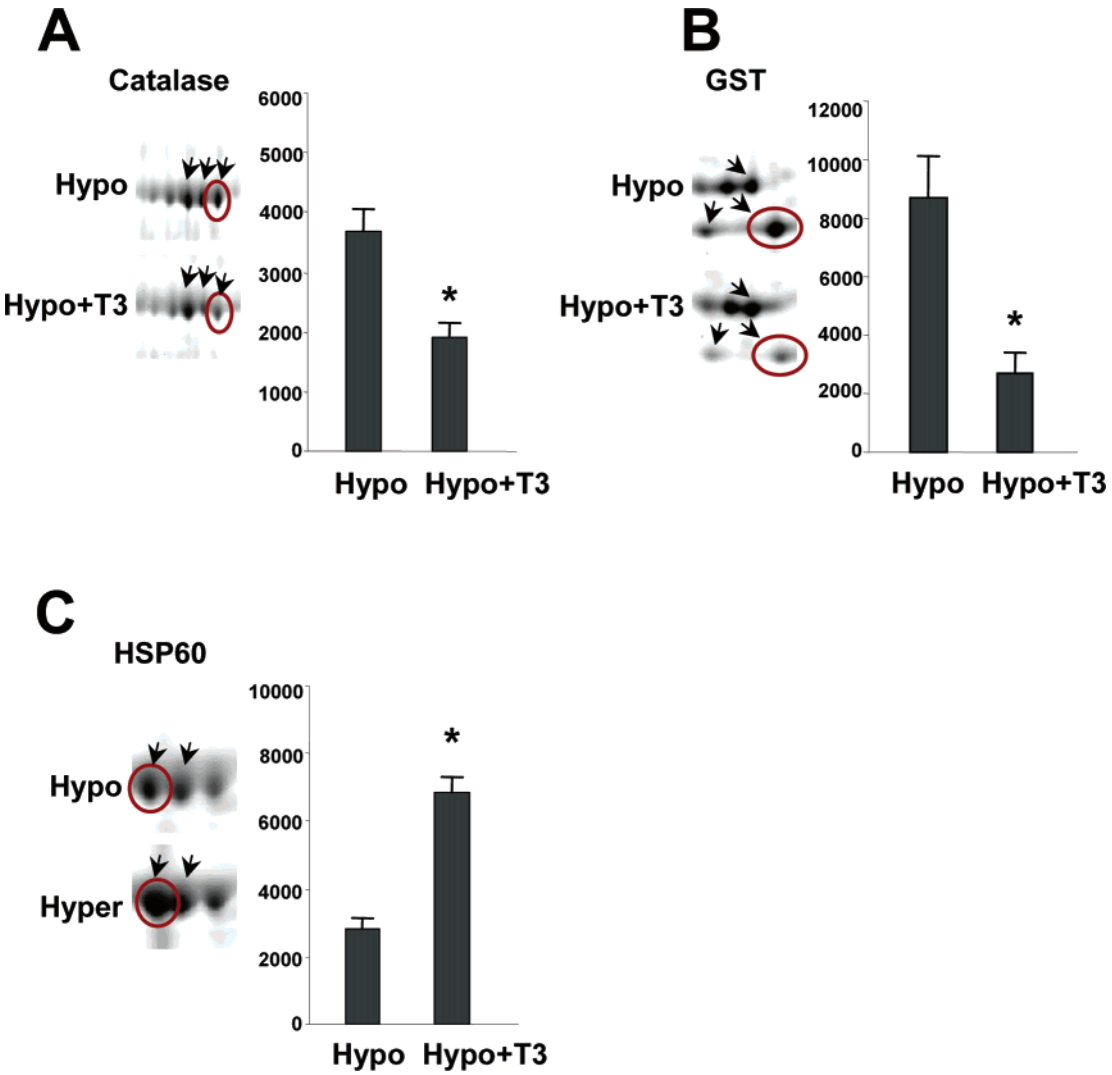

Figure 3. Example of differential expression of liver proteins involved in detoxification of cytotoxic products and stress derangement. Representative subsections of 2D=E images are shown for: (A) catalase; (B) glutathione-S-transferase (GST); (C) heat shock protein 60 (HSP60). In each panel, histograms show means ± SE ($n = 4$) for relative intensities (RI) of the protein spots for Hypo, and Hypo+T3 rats. * $P < 0.05$ vs Hypo. Arrows indicate all spots corresponding to the protein, whereas circles indicate the spot to which histograms refer.

in the expression level of electron-transfer flavoprotein α-subunit (α-ETF), an obligatory electron-acceptor for the reactions catalyzed by several dehydrogenases among which are the acyl-CoA dehydrogenases.[43] Nagao et al.[44] showed that the expressions of SCAD, MCAD, and LCAD and that of α-ETF follow a similar developmental pattern in the rat, and that in the liver dexamethasone strongly suppressed the mRNAs not only for all ACDs but also for α-ETF. Our data support a coordinated action of thyroid hormone on the metabolic pathway in which both kinds of enzymes are involved. Indeed, β-oxidation is involved in the respiratory chain at two stages, the linking of 3-hydroxyacyl-CoA dehydrogenase to complex I via NAD^+/NADH, and that of ACDs to ubiquinone via ETF and its oxidoreductase.[32] Inhibition of either of these stages leads to inhibition of β-oxidation.[45,46] ETF-semiquinone, the partially reduced form of ETF, is a potent inhibitor of ACDs,[47] and so, a reduction in the levels of ETF would functionally prevent the inhibition of ACD and β-oxidation.

Detoxification of Cytotoxic Products. Hyperthyroidism is associated with an acceleration of hepatic respiration primarily by increasing mitochondrial respiratory chain activity and the overall O_2 consumption rate with a concomitant increase in reactive oxygen species (ROS) production at mitochondrial, microsomal, and peroxisomal sites (ref 48 and references within). T3-induced liver free-radicals activity is paralleled by a diminution in antioxidant defenses, leading to increased oxidative stress (ref 48 and references within). Here, we show that T3 treatment is associated with significant reductions in the expression levels of both peroxisomal catalase and cytoplasmatic GST. The former is important in protecting cells from the toxic effects of hydrogen peroxide, while the latter is implicated in the cellular detoxification of a number of xenobiotics by means of their conjugation to reduced glutathione (GSH). Previously, it was reported that, in a different model of rat hypothyroidism, catalase activities decrease.[49,50] Our data, in apparent contrast with such results, raise the possibility that thyroid hormone might exert post-translational modulation of catalase enzyme activity, alongside its transcriptional and translational effects. Indeed, catalase protein was identified at multiple spot positions probably reflecting the occurrence of post-translational modifications. The up-regulation of the hepatic level of mitochondrial aldehyde dehydrogenase, re-

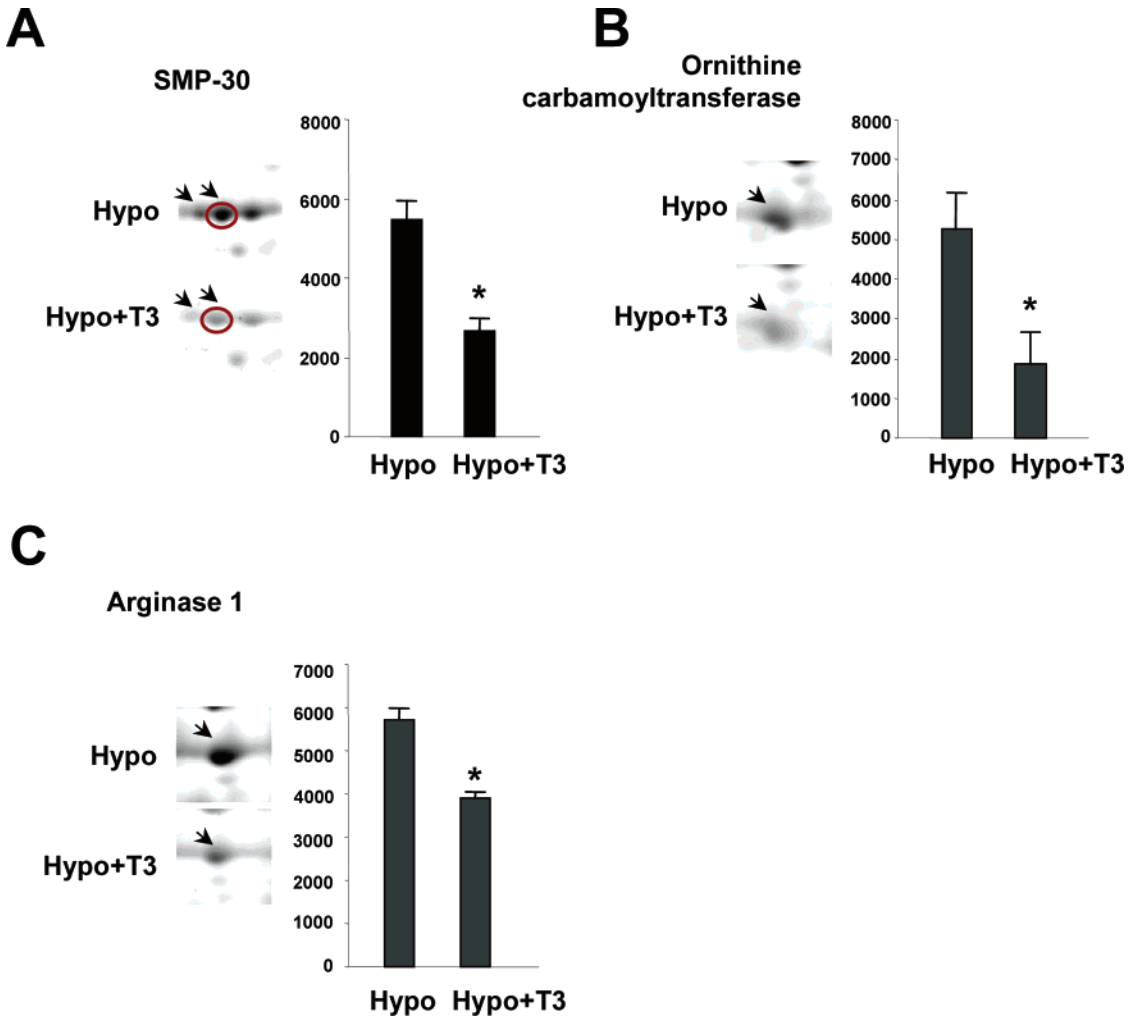

Figure 4. Example of differential expression of liver proteins involved in calcium homeostasis and the urea cycle. Representative subsections of 2D-E images are shown for: (A) senescence marker protein 30 (SMP30); (B) ornithine carbamoyltransferase; (C) arginase 1. In each panel, histograms show means ± SE ($n = 4$) for relative intensities (RI) of the protein spots for Hypo and Hypo+T3 rats. * $P < 0.05$ vs Hypo. Arrows indicate all spots corresponding to the protein, whereas circles indicate the spot to which histograms refer.

ported here, is indicative of increased NADH production via oxidation of aldehydes, reflecting an enhanced scavenging of reactive aldehyde products in the liver following T3 treatment. Moreover, as stated above, we have shown that T3 induces in the liver a significant reduction in the expression of the sorbitol dehydrogenase belonging to the polyolpathway. This, when active, preceding glycolysis: (i) depletes NADPH, concomitantly decreasing GSH levels; (ii) produces NADH, a substrate for oxidase generating ROS; and (iii) leads to potent nonenzymatic glycation agents (such as fructose-3-phosphate and 3-deoxyglucosone) inducing advance formation of glycation end products.[51] Thus, our data seem to suggest that T3, by inhibiting the conversion of sorbitol to fructose, might lead to sorbitol accumulation while, at the same time, counteracting oxidative stress. Once again, down-regulated proteins were identified.

A consequence of the increased oxidative stress imposed on the liver by T3 is an enhancement of lipid peroxidation as well as a promotion of hepatic protein oxidation (ref 48 and references within). Increased ROS, at low concentration, through NADH oxidase activity, have mitogenic potential[52] and could take part of the effect of T3 on cell proliferation.[53]

A possible T3-associated protein oxidation/misfolding and oxidative stress is raised by the selective up-regulation of HSP60, a molecular chaperone. This protein, implicated in mitochondrial protein import and macromolecular assembly, is also known for being able both to prevent misfolding and to promote the refolding of unfolded polypeptides generated under stress conditions.[54,55] Thus, our results support the idea that T3 has a coordinated pattern of action: it accelerates protein import into mitochondria by increasing the expressions of some components of the import machinery,[55] stimulates respiration, and increases ROS production (ref 48 and references within), these, in turn, potentially contributing to its effect on cell proliferation.

Calcium Homeostasis. It has been said that the *primum movens* in some effects of thyroid hormone could be an increase in intracellular calcium.[56] Indeed, T3 is able to induce a redistribution of calcium across plasma and mitochondrial membranes, thereby affecting energy metabolism.[57] SMP30, also known as regucalcin, previously not known to be affected by T3, was here identified as a T3 target. SMP30 plays a pivotal role in the maintenance of intracellular calcium homeostasis due to its activation of calcium-pump enzymes in the plasma membrane, microsomes, and mitochondria of many cell types.[58] In liver, as well as in kidney, heart, and brain, it acts as a multifunctional factor with a suppressive effect on calcium

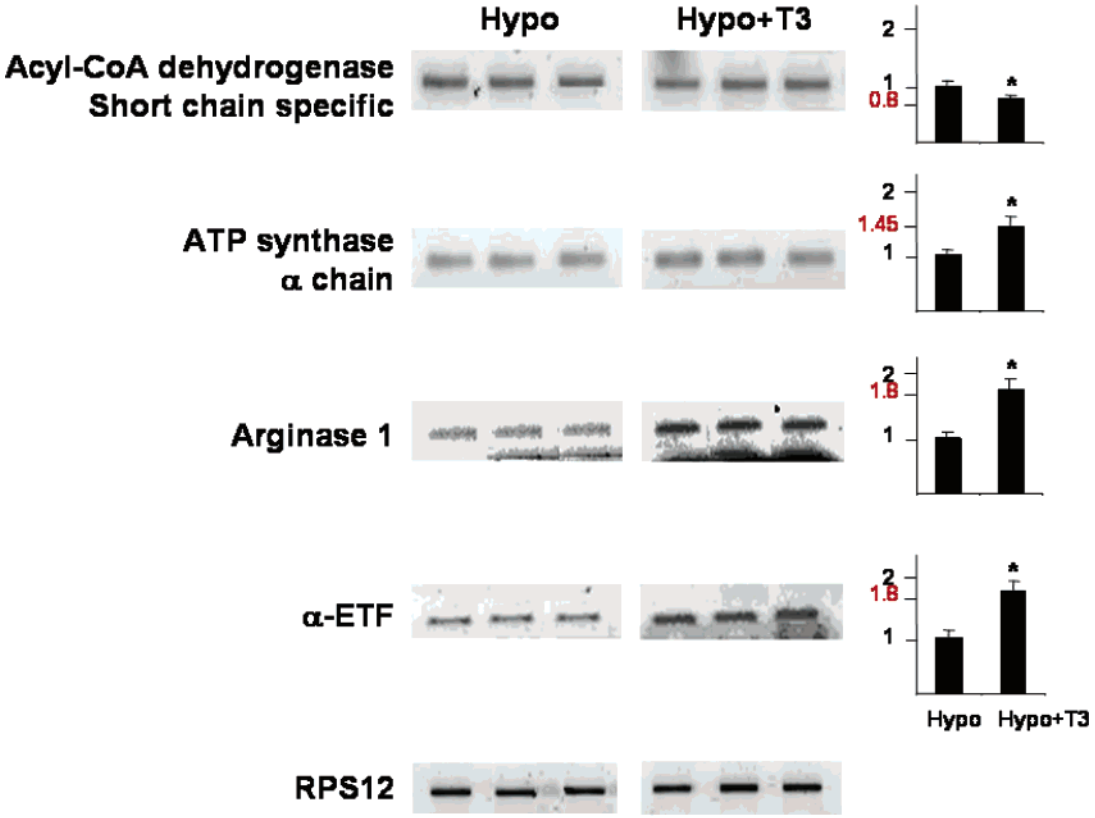

Figure 5. RT-PCR-based measurements of Acyl-CoA dehydrogenase, ATP synthase α chain, Arginase 1, and α-ETF mRNA levels in liver of Hypo and Hypo+T3 rats. RPS12 mRNA levels were measured as the internal standard. Each lane contains PCR product derived from the appropriate cDNA, for which 1 μg of total RNA was used. Each treatment was performed in triplicate. On the right side, quantification of the data. Data are expressed relative to the value obtained for control (Hypo) liver, which is set as 1.0, and are presented separately for each treatment (as indicated below the bars). In red, the fold change Hypo+T3 vs Hypo is reported. Error bars represent SD of the mean (n = 3 rats). * P < 0.05 vs Hypo.

signaling and with the ability to control several cellular functions.[58] In the liver of T3-treated rats, we observed a significant reduction in the SMP30 protein level. The increase in oxidative conditions during aging may play a major role in the reduction in SMP30 expression levels in the liver.[59] Thus, it seems likely that the down-regulation of SMP30 expression by T3 is an effect linked to T3-induced oxidative stress. Such an effect of T3 on SMP30 expression levels opens new perspectives in our understanding of the molecular pathways related to intracellular T3-dependent signaling, raising the possibility that T3 may modulate a plethora of cellular events while also acting on multifunctional proteins such as SMP30, which in turn is able to modulate the levels of second messengers such as calcium.

Amino Acid Catabolism and the Urea Cycle. Hypothyroidism is associated with an increased hepatic capacity to synthesize urea and, thus, with increased ammonia production.[60,61] Here, in the liver of T3-treated rats, we show significant reductions in the protein levels of both ornithine carbamoyltransferase and arginase 1, supporting the idea that in the hyperthyroid state there are decreases in urea and ammonia production.

In an attempt to deeper investigate on the significance of the <2-fold changes observed for some of the identified proteins following T3 treatment, measurements of mRNA expression levels were made. For acyl-CoA dehydrogenase and ATP synthase α-chain, both mRNA and protein expression levels showed a similar trend, while for α-ETF and arginase 1, an increase in mRNA corresponded to a decrease in protein level pointing toward post-translational effects of T3.

Of note, 70% of the identified proteins shown to be differentially expressed in maps from T3-treated rats were down-regulated relative to the hypothyroid condition. Looking at the literature, it is now emerging that negative regulation by T3 might be much more prevalent than previously thought, as transcriptome analyses revealed that T3 exerts both positive and negative regulation within the same cell of many target genes.[62] Moreover, T3 signaling can affect also mRNA and protein stability and translation[9] in a broad context of cellular and molecular events including cell sensitivity to T3, nongenomic effects, and cross-talks with other signaling pathways.[62] In view of such a complexity of thyroid hormone signaling, our proteome analysis data contribute to the knowledge of the cellular pathways affected by T3 even if they do not provide any element concerning the negative modulation of the expression of T3 target genes.

Conclusion

The data reported show for the first time the concomitant effects that T3 elicits in vivo on the expressions of proteins involved in several biochemical/metabolic pathways in the liver. The observed effects could be the result of an action of T3 on several aspects crucial in determining protein levels (i.e., mRNA stability, translation efficiency, protein stability, etc.). Since many of the identified proteins were previously unrecognized as affected by T3 in rat liver, our data offer new insights

in the cellular- and tissue-specific actions of this hormone. However, since this study was performed in vivo, we cannot exclude the possibility that certain hormones and/or other factors that are affected by T3 administration may have played roles in the results obtained here.

Acknowledgment. This work was supported by grants from MIUR-COFIN and Regione Campania.

References

(1) Brent, G. A. The molecular basis of thyroid hormone action. *N. Engl. J. Med.* **1994**, *331* (13), 847−853.

(2) Silvestri, E.; Schiavo, L.; Lombardi, A.; Goglia, F. Thyroid hormones as molecular determinants of thermogenesis. *Acta Physiol. Scand.* **2005**, *184* (4), 265−283.

(3) Lazar, M. A. Thyroid hormone receptors: multiple forms, multiple possibilities. *Endocr. Rev.* **1993**, *14* (2), 184−193.

(4) Lazar, M. A. Thyroid hormone action: a binding contract. *J. Clin. Invest.* **2003**, *112* (4), 497−499.

(5) Yen, P. M.; Chi, W. W. Molecular mechanisms of dominant negative activity by nuclear hormone receptors. *Mol. Endocrinol.* **1994**, *8* (11), 1450−1454.

(6) Goglia, F.; Moreno, M.; Lanni, A. Action of thyroid hormones at the cellular level: the mitochondrial target. *FEBS Lett.* **1999**, *452* (3), 115−120.

(7) Gaspari, M.; Larsson, N. G.; Gustafsson, G. M. The transcription machinery in mammalian mitochondria. *Biochim. Biophys. Acta* **2004**, *1659* (2−3), 148−152.

(8) Scarpulla, R. C. Nuclear control of respiratory gene expression in mammalian cells. *J. Cell. Biochem.* **2005**, *97* (4), 673−683.

(9) Wrutniak-Cabello, C.; Casas, F.; Cabello, G. Thyroid hormone action in mitochondria. *J. Mol. Endocrinol.* **2001**, *26* (1), 67−77.

(10) Koenig, R. J. Thyroid hormone receptor coactivators and corepressors. *Thyroid* **1998**, *8* (8), 703−713.

(11) Davis, P. J.; Davis, F. B. Nongenomic actions of thyroid hormone on the heart. *Thyroid* **2002**, *12*, 459−446.

(12) Soboll, S. Regulation of energy metabolism in liver. *J. Bioenerg. Biomembr.* **1995**, *27* (6), 571−582.

(13) Oppenheimer, J. H.; Schwartz, H. L.; Mariash, C. N.; Kinlaw, W. B.; Wong, N. C.; Freake, H. C. Advances in our understanding of thyroid hormone action at the cellular level. *Endocr. Rev.* **1987**, *8* (3), 288−308.

(14) Feng, X.; Jiang, Y.; Meltzer, P.; Yen, P. M. Thyroid hormone regulation of hepatic genes in vivo detected by complementary DNA microarray. *Mol. Endocrinol.* **2000**, *14* (7), 947−955.

(15) Weitzel, J. M.; Radtke, C.; Seitz, H. J. Two thyroid hormone-mediated gene expression patterns in vivo identified by cDNA expression arrays in rat. *Nucleic Acids Res.* **2001**, *29* (24), 5148−5155.

(16) Fountoulakis, M. Proteomics: current technologies and applications in neurological disorders and toxicology. *Amino Acids* **2001**, *21* (4), 363−381.

(17) Righetti, P. G.; Castagna, A.; Antonucci, F.; Piubelli, C.; Cecconi, D.; Campostrini, N.; Rustichelli, C.; Antonioli, P.; Zanusso, G.; Monaco, S.; Lomas, L.; Boschetti, E. Proteome analysis in the clinical chemistry laboratory: myth or reality? *Clin. Chim. Acta* **2005**, *357* (2), 123−139.

(18) Moreno, M.; Lanni, A.; Lombardi, A.; Goglia, F. How the thyroid controls metabolism in the rat: different roles for triiodothyronine and diiodothyronines. *J. Physiol.* **1997**, *505* (Pt 2), 529−538.

(19) Lanni, A.; Moreno, M.; Lombardi, A.; Goglia, F. Calorigenic effect of diiodothyronines in the rat. *J. Physiol. (London, U.K.)* **1996**, *494*, 831−837.

(20) Freake, H. C.; Schwartz, H. L.; Oppenheimer, J. H. The regulation of lipogenesis by thyroid hormone and its contribution to thermogenesis. *Endocrinology* **1989**, *125*, 2868−2874.

(21) Fountoulakis, M.; Suter, L. Proteomic analysis of the rat liver. *J. Chromatogr., B: Anal. Technol. Biomed. Life Sci.* **2002**, *782* (1−2), 197−218.

(22) Bradford, M. M. A rapid and sensitive method for the quantitation of microgram quantities of protein utilizing the principle of protein-dye binding. *Anal. Biochem.* **1976**, *72*, 248−254.

(23) Fountoulakis, M.; Langen, H. Identification of proteins by matrix-assisted laser desorption ionization-mass spectrometry following in-gel digestion in low-salt, nonvolatile buffer and simplified peptide recovery. *Anal. Biochem.* **1997**, *250* (2), 153−156.

(24) Magnuson, M. A.; Nikodem, V. M. Molecular cloning of a cDNA sequence for rat malic enzyme. Direct evidence for induction in vivo of rat liver malic enzyme mRNA by thyroid hormone. *J. Biol. Chem.* **1983** *258* (20), 12712−12717.

(25) Kohrle, J.; Schomburg, L.; Drescher, S.; Fekete, E.; Bauer, K. Rapid stimulation of type I 5′-deiodinase in rat pituitaries by 3,3′,5-triiodo-L-thyronine. *Mol. Cell. Endocrinol.* **1995** *108* (1−2), 17−21.

(26) Rout, U. K.; Holmes, R. S. Alcohol dehydrogenases and aldehyde dehydrogenases among inbred strains of mice: multiplicity, development, genetic studies and metabolic roles. *Addict. Biol.* **1996**, *1* (4), 349−362.

(27) Crabb, D. W.; Matsumoto, M.; Chang, D.; You, M. Overview of the role of alcohol dehydrogenase and aldehyde dehydrogenase and their variants in the genesis of alcohol-related pathology. *Proc. Nutr. Soc.* **2004**, *63* (1), 49−63.

(28) Li, J.; French, B. A.; Fu, P.; French, S. W. Liver necrosis induced by thyroid hormone administration in rats fed ethanol. *Exp. Mol. Pathol.* **2001**, *71* (1), 79−88.

(29) Li, J.; Nguyen, V.; French, B. A.; Parlow, A. F.; Su, G. L.; Fu, P.; Yuan, Q. X.; French, S. W. Mechanism of the alcohol cyclic pattern: role of the hypothalamic-pituitary-thyroid axis. *Am. J. Physiol.: Gastrointest. Liver Physiol.* **2000**, *279* (1), G118−G125.

(30) Muller, M. J.; Thomsen, A.; Sibrowski, W.; Seitz, H. J. 3,5,3′-Triiodothyronine-induced synthesis of rat liver phosphoenolpyruvate carboxykinase. *Endocrinology* **1982**, *111*, 1469−1475.

(31) Merkulova, T.; Keller, A.; Oliviero, P.; Marotte, F.; Samuel, J. L.; Rappaport, L.; Lamande, N.; Lucas, M. Thyroid hormones differentially modulate enolase isozymes during rat skeletal and cardiac muscle development. *Am. J. Physiol.: Endocrinol. Metab.* **2000**, *278* (2), E330−E339.

(32) Moeller, L. C.; Dumitrescu, A. M.; Walker, R. L.; Meltzer, P. S.; Refetoff, S. Thyroid hormone responsive genes in cultured human fibroblasts. *J. Clin. Endocrinol. Metab.* **2005**, *90* (2), 936−943.

(33) Shinohara, R.; Mano, T.; Nagasaka, A.; Sawai, Y.; Uchimura, K.; Hayashi, R.; Hayakawa, N.; Nagata, M.; Makino, M.; Kakizawa, H.; Itoh, Y.; Nakai, A.; Itoh, M. Effects of thyroid hormone on the sorbitol pathway in streptozotocin-induced diabetic rats. *Biochim. Biophys. Acta* **1998**, *1425* (3), 577−586.

(34) Heimberg, M.; Olubadewo, J. O.; Wilcox, H. G. Plasma lipoproteins and regulation of hepatic metabolism of fatty acids in altered thyroid states. Plasma lipoproteins and regulation of hepatic metabolism of fatty acids in altered thyroid states. *Endocr. Rev.* **1985**, *6* (4), 590−607.

(35) Ghisla, S.; Thorpe, C. Acyl-CoA dehydrogenases. A mechanistic overview. *Eur. J. Biochem.* **2004,** *271*(3), 494−508.

(36) Eaton, S.; Bartlett, K.; Pourfarzam, M. Mammalian mitochondrial β-oxidation. *Biochem. J.* **1996**, *320*, 345−357.

(37) Davidson, B.; Schulz, H. Separation, properties, and regulation of acyl coenzyme A dehydrogenases from bovine heat and liver. *Arch. Biochem. Biophys.* **1982**, *213* (1), 155−162.

(38) Powell, P. J.; Lau, S. M.; Killian, D.; Thorpe, C. Interaction of acyl coenzyme A substrates and analogues with pig kidney medium-chain acyl-coA dehydrogenase. *Biochemistry* **1987**, *26* (12), 3704−3710.

(39) Schifferdecker, J.; Schulz, H. The inhibition of L-3-hydroxyacyl-CoA dehydrogenase by acetoacetyl-CoA and the possible effect of this inhibitor on fatty acid oxidation. *Life Sci.* **1974**, *14* (8), 1487−1492.

(40) Lanni, A.; Moreno, M.; Lombardi, A.; Goglia, F. Thyroid hormone and uncoupling proteins. *FEBS Lett.* **2003**, *543* (1−3), 5−10.

(41) Goglia, F.; Silvestri, E.; Lanni, A. Thyroid hormones and mitochondria. *Biosci. Rep.* **2002**, *22* (1), 17−32.

(42) Lanni, A.; Moreno, M.; Lombardi, A.; de Lange, P.; Goglia, F. Control of energy metabolism by iodothyronines. *J. Endocrinol. Invest.* **2001**, *24* (11), 897−913.

(43) Crane, F.l.; Beinert, H. On the mechanism of dehydrogenation of fatty acyl derivatives of coenzyme A. II. The Electron-Transferring Flavoprotein. *J. Biol. Chem.* **1956**, *218* (2), 717−731.

(44) Nagao, M.; Parimoo, B.; Tanaka, K. Developmental, nutritional, and hormonal regulation of tissue-specific expression of the genes encoding various acyl-CoA dehydrogenases and alpha-subunit of electron-transfer flavoprotein in rat. *J. Biol. Chem.* **1993**, *268* (32), 24114−24124.

(45) Bremer, J.; Wojtczak, A. B. Factors controlling the rate of fatty acid oxidation in rat liver mitochondria. *Biochim. Biophys. Acta* **1972**, *280* (4), 515−530.

(46) Kler, R. S.; Jackson, S.; Bartlett, K.; Bindoff, L. A.; Eaton, S.; Pourfarzam, M.; Frerman, F. E.; Goodman, S. I.; Watmough, N. J.; Turnbull, D. M. Quantitation of acyl-CoA and acylcarnitine esters accumulated during abnormal mitochondrial fatty acid oxidation. *J. Biol. Chem.* **1991**, *266* (34), 22932−22938.
(47) Beckmann, J. D.; Frerman, F. E.; McKean, M. C. Inhibition of general acyl CoA dehydrogenase by electron-transfer flavoprotein semiquinone. *Biochem. Biophys. Res. Commun.* **1981**, *102* (4), 1290−1294.
(48) Videla, L. A. Energy metabolism, thyroid calorigenesis, and oxidative stress: functional and cytotoxic consequences. *Redox Rep.* **2000**, *5* (5), 265−275.
(49) Yilmaz, S.; Ozan, S.; Benzer, F.; Canatan, H. Oxidative damage and antioxidant enzyme activities in experimental hypothyroidism. *Cell Biochem. Funct.* **2003**, *21* (4), 325−330.
(50) Ichikawa, K.; Hashizume, K.; Yamada, T.; Hashimoto, T. Effect of thyroid hormone on peroxisomal flavin enzymes in rat liver and kidney. *Endocrinol. Jpn.* **1987**, *34* (2), 245−250.
(51) Lee, A. Y. W.; Chung, S. S. M. Contributions of polyol pathway to oxidative stress in diabetic cataract. *FASEB J.* **1999**, *13* (1), 23−30.
(52) Thannickal, V. J.; Day, R. M.; Klinz, S. G.; Bastien, M. C.; Larios, J. M.; Fanburg, B. L. Ras-dependent and -independent regulation of reactive oxygen species by mitogenic growth factors and TGF-beta1. *FASEB J.* **2000**, *14* (12), 1741−1748.
(53) Columbano, A.; Pibiri, M.; Deidda, M.; Cossu, C.; Scanlan, TS.; Chiellini, G.; Muntoni, S.; Ledda-Columbano, G. M. The thyroid hormone receptor-{Beta} agonist Gc-1 induces cell proliferation in rat liver and pancreas. *Endocrinology* **2006**, *147* (7), 3211−3218.
(54) Hood, D. A.; Joseph, A. M. Mitochondrial assembly: protein import. *Proc. Nutr. Soc.* **2004**, *63* (2), 293−300.
(55) Hood, D. A.; Adhihetty, P. J.; Colavecchia, M.; Gordon, J. W.; Irrcher, I.; Joseph, A. M.; Lowe, S. T.; Rungi, A. A. Mitochondrial biogenesis and the role of the protein import pathway. *Med. Sci. Sports Exercise* **2003**, *35* (1), 86−94.
(56) Segal, J.; Ingbar, S. H. Evidence that an increase in cytoplasmic calcium is the initiating event in certain plasma membrane-mediated responses to 3,5,3′-triiodothyronine in rat thymocytes. *Endocrinology* **1989**, *124* (4), 1949−1955.
(57) D'Arezzo, S.; Incerpi, S.; Davis, F. B.; Acconcia, F.; Marino, M.; Farias, R. N.; Davis, P. J. Rapid nongenomic effects of 3,5,3′-triiodo-L-thyronine on the intracellular pH of L-6 myoblasts are mediated by intracellular calcium mobilization and kinase pathways. *Endocrinology* **2004**, *145* (12), 5694−5703.
(58) Yamaguchi, M. Role of regucalcin in maintaining cell homeostasis and function. *Int. J. Mol. Med.* **2005**, *15* (3), 371−389.
(59) Jung, K. J.; Ishigami, A.; Maruyama, N.; Takahashi, R.; Goto, S.; Yu, B. P.; Chung, H. Y. Modulation of gene expression of SMP-30 by LPS and calorie restriction during aging process. *Exp. Gerontol.* **2004**, *39* (8), 1169−1177.
(60) Marti, J.; Portoles, M.; Jimenez-Nacher, I.; Cabo, J.; Jorda, A. Effect of thyroid hormones on urea biosynthesis and related processes in rat liver. *Endocrinology* **1988**, *123* (5), 2167−2174.
(61) Sochor, M.; McLean, P.; Brown, J.; Greenbaum, A. L. Regulation of pathways of ornithine metabolism. Effects of thyroid hormone and diabetes on the activity of enzymes at the "ornithine crossroads" in rat liver. *Enzyme* **1981**, *26* (1), 15−23.
(62) Flamant, F.; Gauthier, K.; Samarut, J. Thyroid hormones signaling is getting more complex: STORMs are coming. *Mol. Endocrinol.* **2006**, published online Jun 8, http://dx.doi.org/doi:10.1210/me.2006-0035.

PR060141L